Published in IET Signal Processing
Received on 10th August 2009
Revised on 29th December 2009
doi: 10.1049/iet-spr.2009.0203

ISSN 1751-9675

Human elbow joint angle estimation using electromyogram signal processing

H.-J. Yu[1] *A.Y. Lee*[2] *Y. Choi*[2]

[1]*LS MTRON, Anyang 431-080, Republic of Korea*
[2]*Electronic, Electrical, Control and Instrumentation Engineering, Hanyang University, 426-791, Republic of Korea*
E-mail: cyj@hanyang.ac.kr

Abstract: This study proposes a real-time joint angle estimation method of human elbow by processing a biomedical signal of surface synergistic EMG (electromyogram) measured between biceps brachii and triceps brachii simultaneously. Actually, the EMG is known as a non-stationary signal, but the authors assume that it is quasi-stationary because a physical or physiological system has limitations in the rate at which it can change its characteristics. Based on the assumption, a pre-processing method to obtain pre-angle values from the raw synergistic EMG signal is firstly suggested, and then a method to estimate the joint angle through normalisation when there are external loads is discussed. In addition, an optimisation method to minimise the error between the normalised angle and real joint angle is proposed. Finally, the authors show the effectiveness of the suggested algorithm through experimental results.

1 Introduction

There have been many researches about biomedical signal processing methodologies in [1–15]. As a matter of fact, the human body generates various bioelectrical signals such as ECG (electrocardiogram), EEG (Electroencephalogram: popularly known as brain waves), EMG (Electromyogram) etc. [1]. Among these kinds of bioelectrical signals, the EMG signal has been actively studied for the human muscle analysis and motion imitation in robotics and rehabilitation engineering [2–11, 14, 15]. Especially, the EMG signal has been one of the best candidates in developing a bio-mechanical system by transferring the robotics technologies to the rehabilitation ones. In the areas of robotics and control engineering using the EMG signal processing, most researches have been focusing on the development of a prosthetic device for the disabled.

Cavallaro *et al.* developed a myoprocessor based on the Hill phenomenological muscle model in [2]. Bitzer *et al.* and Nishikawa *et al.* developed the prosthetic hands using learning methods in [3, 4], respectively. Zhao *et al.* presented a surface EMG motion pattern classifier which combines Levenberg–Marquardt (LM)-based neural network with parametric autoregressive (AR) model in [5]. In the EMG pattern recognitions, many kinds of methods have been developed so as to extract a variety of features such as integral absolute value (IAV), variance and zero crossing from the measured EMG signal in [6]. Although the EMG signals have often been used as a part of control signals for prosthetic hands, these prosthetic hands are seldom used by the amputee because they require the light devices in weight and the precise motion/force estimation from EMG signals in realtime. As an alternative of these problems, Fukuda *et al.* proposed a novel statistical neural network called the log-linearised Gaussian mixture network (LLGMN) and a human-assisting manipulator system tele-operated by EMG signals and arm motion sensors in [7]. Also, the ARMAX (auto-regressive moving average with exogenous output) model has been used for the tele-operation by the EMG signal processing in [8]. Morita *et al.* proposed a direct torque control method using the feedback error learning scheme for the prosthetic hand in [9]. Recently, Su *et al.* developed an EMG-controlled 3-D graphical prosthetic hand using a 3-D electromagnetic positioning system in [10]. They classified the EMG patterns corresponding to the hand motions using a data-glove with 11 miniature electromagnetic sensors. Also, many adaptive methods have been developed to cancel the noises presented in the biomedical signals in [12, 13]. Winter carried out a research about a generation of a force according to a modelling of muscle through the analysis of a motor unit of muscle-fibre in [16]. Doheny *et al.* analysed a relationship between the force and the EMG signal according to a maximum voluntary contraction (MVC) after measuring the EMG signal at various angles of the human elbow joint in [17]. Artemiadis *et al.* estimated the force from the EMG signal through constructing a spring model coupled with a human arm and a robot arm in [18]. Ito *et al.* suggested a method to control a prosthetic arm using the pattern classification of the EMG signal in [19]. Besides the above researches, there have been many researches about analysing the relationship between the EMG signal and the force in [20–23]. As aforementioned, although there have been many kinds of researches on the pattern

classification and recognition methods of human motion using the neural network, it has hardly been studied for the direct extraction method of joint angle from the EMG signal itself which is generated according to the human motion.

In this paper, we propose a real-time elbow joint angle extraction method from the surface EMG signals, which are synergistic signals acquired simultaneously between the biceps muscle and the triceps muscle. Additionally, we discuss a method to extract the elbow joint angle when applying the external loads. In the first place, we assume that the EMG signal is quasi-stationary, in fact, most biomedical systems are dynamic and produce non-stationary signals, but a physical or physiological system has limitations in the rate at which it can change its characteristics [1]. This limitation facilitates breaking a signal into segments of short duration, over which the statistics of interest are not varying or may be assumed to remain the same. Actually, the meaning of segments of short duration varies according to subjects; for example, some subjects are able to keep up the stationary results for a few minutes, but some does not keep them even for a few seconds because it depends on the physical state of the subjects. Thus, we assume that the muscle fatigue is excluded, in other words, if the subject feels the muscle fatigue, then the subject should take rest before getting restated the experiments. Then, the corresponding signal can be referred to as a quasi-stationary one.

The proposed algorithm consists of two processing stages: pre-processing and optimisation process. In the pre-processing, the signals are processed by taking the root-mean-squares (RMS) in a given period of moving window, filtering noises out with low-pass filter (LPF) and making polynomial interpolation given a few data. Then, the pre-angle values are obtained kinematically for elbow joint angles. Additionally, the pre-angle values are normalised when applying external loads. As a second stage, the optimisation process is proposed by using Lagrange multiplier method for the minimisation of a given performance index. Finally, the processed signals are directly used for the real-time motion tracking of elbow joint, in other words, we suggest the real-time motion tracking algorithm which follows the flexion and extension motion of a human elbow joint well.

This paper is organised as follows: section 2 proposes the pre-processing method to obtain the normalised-angle values; Section 3 suggests the optimisation process to acquire more precise joint angle estimations; section 4 summarises an entire algorithm as sequential steps for implementations; section 5 shows the validity of the suggested algorithms through experimental results and Section 6 presents the conclusion. For future notation, the L_2-norm of error is defined with a sampling time T as follows:

$$\|e\|_2 = \frac{1}{(m+1)T}\sqrt{\sum_{n=0}^{m} e[n]^2 T}$$

2 Pre-processing

In this section, a pre-processing method is suggested to obtain a normalised angle that will be used in optimisation process later. In general, the EMG signal has some features as follows: firstly, each person has his/her own EMG signal amplitude and frequency characteristics; secondly, even though it is the EMG signal measured from the same person, the characteristics of the EMG signal may become different according to the physical condition of human body, the attachment points of electrodes and the environmental condition such as the temperature [1, 3, 4, 11, 17] when acquiring the EMG signal. It is not possible to acquire the same EMG signal each time because of the various factors attributed to the change of the EMG signal. As an alternative of these problems, it is necessary to take the pre-processing to be suggested for matching the elbow joint angles with the characteristics of the acquired EMG signals.

The pre-processing procedures consist of taking the RMS in a given period of moving window, filtering noises out with LPF (low-pass filter), and making polynomial interpolation given a few data. And then, the pre-angle and normalised angle values are obtained kinematically for elbow joint angles. Before explaining the pre-processing, let us consider the kinematic characteristics of human elbow joint. The human elbow joint motion is defined as flexion and extension, also the range of motion of elbow joint is known as about $0-145^\circ$. Actually, there may be a hyperextension of about 0 to 5° when humans attempt to be over-extended their own forearms [24]. In general, since the hyperextension is relatively very small, we are to exclude the hyperextension for simplification of the algorithm development. A power source muscle of flexion motion is the biceps brachii and that of extension motion is the triceps brachii in the anatomical terminology. In this paper, we will focus on the synergistic EMG signal, which is acquired using bipolar snap electrodes by attaching one of the both electrodes on the biceps brachii and another on the triceps brachii.

The flexion motion is occurred by the cooperative activations of biceps brachii, brachialis, brachioradialis and pronator teres [24]. Also, the extension motion is occurred by the cooperative activations of triceps brachii and anconeus [24]. However, in the case of the forearm amputee, it is impossible to acquire the signals of brachioradialis, the pronator teres and anconeus since they are all placed into the forearm amputated. Furthermore, even though for the normal person it is difficult to acquire the EMG signal directly from the brachialis using the surface electrodes because most parts of the brachialis are covered with the biceps brachii. As aforementioned reasons, we have selected both biceps and triceps muscles for acquiring the synergistic EMG signal. In addition, since the EMG signal is sensitive to various environmental conditions, the attachment points of electrodes become very important for precise signal acquisition. Thus, we try to attach the electrodes to the centre of motor point of biceps brachii and triceps brachii, respectively. Also, we make use of Ag/AgCl one time electrodes which are widely used for the precise biomedical signal acquisition.

2.1 Taking RMS and LPF

First, we set the sampling frequency to 1024 Hz, for the experimental equipment offers EMG data with the maximum rate of 1024 sample/s. Fig. 1*a* shows the raw synergistic EMG signals acquired from flexion first and then extension according to time progress (1024 samples = 1 s). As we can see in Fig. 1*a*, the sequential flexion and extension motions have something to do with the amplitude of signal. More concretely, the maximum amplitude increases as the elbow joint angle increases,

doi: 10.1049/iet-spr.2009.0203

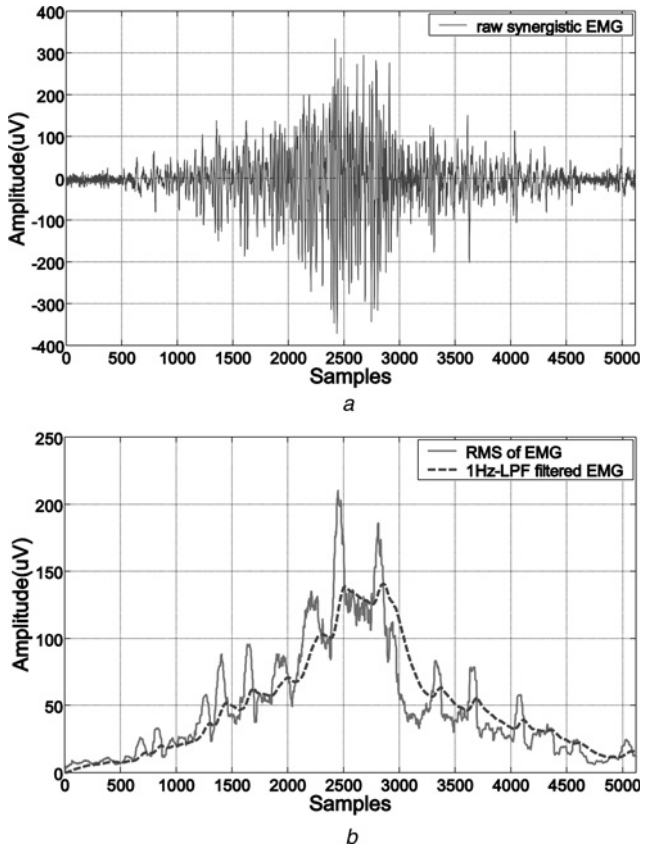

Fig. 1 *Signals obtained by taking RMS and LPF*

a EMG signal acquired from flexion first and then extension motion
b RMS signal taken through a given moving window of 64 samples and LPF signal obtained using the cut-off frequency 1 Hz

though they do not seem to be linear. This property will be discussed in the following section.

Now, we take RMS value with 64 samples moving window to obtain the average envelope information approximately in the following form

$$\mathrm{RMS}[n] = \sqrt{\frac{1}{64}\sum_{k=n-63}^{n} EMG[k]^2} \quad \text{for} \quad n = 0, 1, \ldots, m \tag{1}$$

where $RMS[n]$ is the RMS value obtained from 64 samples moving window and $EMG[k]$ the raw synergistic EMG signal at kth sample with $EMG[k] = 0$ for $k = -63, -62, \ldots, -1$. As a matter of fact, the RMS value of signal includes the information of muscle power as well as the envelope [1]. As solid lines shown in Fig. 1*b*, the RMS values show the similar characteristics with positive envelope of EMG signal.

As a next step, we take the LPF to RMS signal, because the human elbow motion has the bandwidth of at most a few Hertz, in the following form

$$\mathrm{LPF}[n] = \theta \mathrm{RMS}[n] + (1-\theta)\mathrm{LPF}[n-1] \quad \text{for } n = 0, 1, \ldots, m \tag{2}$$

where $\mathrm{LPF}[n]$ is the low-pass-filtered signal at nth sample with $\mathrm{LPF}[-1] = 0$ and θ is defined as follows

$$\theta = 2\pi f_c T \tag{3}$$

where T is a sampling period of 1/1024(s) and f_c is a cut-off frequency in (Hz) for low-pass filtering, here, $f_c = 1$, actually, (2) is the simple discrete form of LPF obtained by applying the forward difference rule to the continuous LPF. The corresponding LPF signals are shown as dashed lines in Fig. 1*b*. By taking LPF, we can obtain the smooth signal for the flexion and extension motion of elbow joint. These LPF signals will be used for the pre-angle generation suggested in the following section.

2.2 Pre-angle generation

The pre-angle generation method is based on the curve fitting using polynomial interpolation. In other words, after keeping a given specific elbow joint angle for short duration, we obtain the averages of LPF values of (2) in the following form

$$V_{\mathrm{LPF}}[q_i] = \frac{1}{L+1}\sum_{k=0}^{L} \mathrm{LPF}[k] \quad \text{for } k = 0, 1, \ldots, L \tag{4}$$

where $V_{\mathrm{LPF}}[q_i]$ is the average of LPF values at a specific joint angle q_i and i is the number of specific joint angles. For example, at four specific joint angles of 0°, 45°, 90° and 145°, the averages of LPF values can be obtained with fixed 512 (samples) as shown in Fig. 2. Fig. 2 was obtained from the experiments about one subject. The following data obtained from Fig. 2 show that the average low-pass-filtered RMS value increases as the elbow joint angle increases

$$V_{\mathrm{LPF}}[0^\circ] = 5.2618 \rightarrow V_{\mathrm{LPF}}[45^\circ] = 10.4527 \rightarrow V_{\mathrm{LPF}}[90^\circ] = 20.9107 \rightarrow V_{\mathrm{LPF}}[145^\circ] = 42.6719$$

In addition, we can know that the maximum amplitude increases as the elbow joint angle increases from Fig. 2, although they do not have the linear proportional relation. With four given data set, the polynomial interpolation can be implemented for third-order polynomial function in the

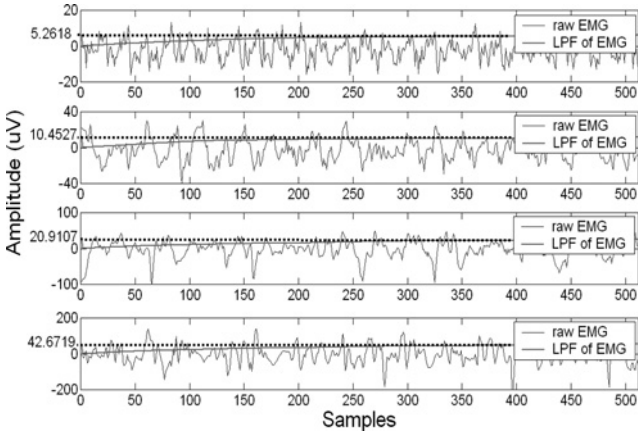

Fig. 2 *Example of one subject*

The first sub-figure shows $V_{\mathrm{LPF}}[0^\circ]$ at the specific angle 0°, the second shows V_{LPF} [45°] at the specific angle 45°, the third shows $V_{\mathrm{LPF}}[90^\circ]$ at the specific angle 90° and the last shows $V_{\mathrm{LPF}}[145^\circ]$ at the specific angle 145° (in the above figures, the dotted lines are $V_{\mathrm{LPF}}[q_i]$)

following form

$$q_i = a_0 + a_1 V_{\mathrm{LPF}}[q_i] + a_2 V_{\mathrm{LPF}}[q_i]^2 + a_3 V_{\mathrm{LPF}}[q_i]^3 \quad (5)$$

where a_0, a_1, a_2, a_3 are the coefficients to be determined by using given data set obtained at four specific joint angles of 0°, 45°, 90° and 145°.

Now, a scaling function between the LPF value and a pre-angle of elbow joint can be obtained. As a result, the pre-angle is generated in real time by using the coefficients determined from polynomial interpolation in the following form

$$x[n] = a_0 + a_1 \mathrm{LPF}[n] + a_2 \mathrm{LPF}[n]^2 + a_3 \mathrm{LPF}[n]^3 \quad (6)$$

where $x[n]$ is the pre-angle of elbow joint calculated at nth sample and LPF$[n]$ is obtained by (2).

2.3 Normalisation

The pre-angle is generated under no external load condition. If the external loads are applied to the forearm, it is necessary to generate the pre-angle corresponding to the external load change. Therefore we generate the normalised angle through the normalisation of the pre-angle with respect to the reference state (no external load).

First, we obtain the EMG signals at each normally 145° maximum range of flexion (MROF) of the elbow when applying various external loads. By using the amplitude values of these EMG signals, we obtain the ratio of the EMG signal with respect to the reference state as follows

$$\frac{\mathrm{EMG}_{\max}}{\mathrm{EMG}_{\mathrm{ref}}} = \mathrm{Load\_Factor} \quad (7)$$

where $\mathrm{EMG}_{\max}$ is the value of V_{LPF}[MROF] measured at MROF according to the applied external load and $\mathrm{EMG}_{\mathrm{ref}}$ is the V_{LPF}[MROF] measured at MROF of the reference state. Then, we redefine $V_{\mathrm{LPF}}[q_i]$ for determining the unknown coefficients in (5) as follows

$$\frac{V_{\mathrm{LPF}}[q_i]}{\mathrm{EMG}_{\mathrm{ref}}} = V_{\mathrm{nor}}[q_i] \quad (8)$$

where $V_{\mathrm{nor}}[q_i]$ is the normalised value with respect to the reference state. Also, the coefficients in (5) should be newly determined at the reference state using the following equation

$$q_i = a_0 + a_1 V_{\mathrm{nor}}[q_i] + a_2 V_{\mathrm{nor}}[q_i]^2 + a_3 V_{\mathrm{nor}}[q_i]^3 \quad (9)$$

where a_0, a_1, a_2, a_3 are the coefficients to be determined by using given data set obtained at four specific joint angles of 0°, 45°, 90° and MROF (normally 145°) at the reference state. Since we know both the load factor of (7) and the new coefficients of (9) with respect to the reference state, we can normalise the input value LPF$[n]$ with respect to the reference state in (6).

$$\frac{\mathrm{LPF}[n]}{\mathrm{EMG}_{\mathrm{ref}} \times \mathrm{Load\_Factor}} = \mathrm{LPF}_{\mathrm{nor}}[n] \quad (10)$$

where the denominator implies the $\mathrm{EMG}_{\max}$, also we should notice that $\mathrm{EMG}_{\max} = \mathrm{EMG}_{\mathrm{ref}}$ in the case of no load.

Finally, it is possible to extract the elbow joint angle according to the applied external load by using the normalised input value $\mathrm{LPF}_{\mathrm{nor}}[n]$ as follows

$$x_{\mathrm{nor}}[n] = a_0 + a_1 \mathrm{LPF}_{\mathrm{nor}}[n] + a_2 \mathrm{LPF}_{\mathrm{nor}}[n]^2 + a_3 \mathrm{LPF}_{\mathrm{nor}}[n]^3 \quad (11)$$

where $x_{\mathrm{nor}}[n]$ implies the normalised angle. The normalised angle is the resultant signal of pre-processing procedure and it will be used as an input signal of the optimisation process to minimise the tracking error in the following section. In addition, we should note that the proposed pre-processing method can be implemented in real time with 64 samples (or 62.5 ms) delays because the RMS requires 63 samples delays and the LPF requires 1 sample delay.

3 Optimisation process

The normalised-angle generation method suggested in the previous section can be directly used for real time motion tracking of elbow joint; however, it does not guarantee the minimum error between the normalised angle and real elbow joint angle. In this section, we are to solve the optimisation problem for error minimisation with a constraint. Here, we assume that the joint angle to be estimated has the second-order dynamics relation with normalised angle in the following form

$$q[n] = \sum_{k=0}^{2} w_k[n] x_{\mathrm{nor}}[n-k]$$

where $q[n]$ is the elbow joint angle estimate, $x_{\mathrm{nor}}[n]$ is the normalised angle obtained from (11) and $w_k[n]$ expresses the tap weights for $k = 0, 1, 2$ at nth sample. The above equation can be expressed as a vector form

$$q[n] = \boldsymbol{w}(\boldsymbol{n})^{\mathrm{T}} \boldsymbol{x}_{\boldsymbol{nor}}(\boldsymbol{n}) \quad (12)$$

where

$$\boldsymbol{w}(\boldsymbol{n}) = [w_0[n] \quad w_1[n] \quad w_2[n]]^{\mathrm{T}} \quad (13)$$

$$\boldsymbol{x}_{\boldsymbol{nor}}(\boldsymbol{n}) = [x_{\mathrm{nor}}[n] \quad x_{\mathrm{nor}}[n-1] \quad x_{\mathrm{nor}}[n-2]]^{\mathrm{T}} \quad (14)$$

with $x_{\mathrm{nor}}[-1] = x_{\mathrm{nor}}[-2] = 0$. Also, we utilise the tilt sensor during the optimisation process to update the tap weights for minimising a tracking error.

As we can see in Fig. 3, the tracking error between the elbow joint angle estimate of (12) and the angle measured from the tilt sensor attached to the wrist is defined in the

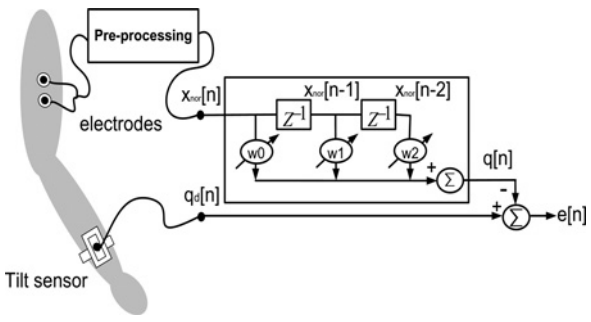

Fig. 3 *Optimisation process*

doi: 10.1049/iet-spr.2009.0203

following form

$$e[n] = q_d[n] - q[n] = q_d[n] - \boldsymbol{w}(\boldsymbol{n})^{\mathrm{T}}\boldsymbol{x}_{\boldsymbol{nor}}(\boldsymbol{n}) \quad (15)$$

where $e[n]$ is the tracking error and $q_d[n]$ is the measured elbow joint angle from the tilt sensor. Also, the minimisation of the rate of tap-weight change is required to avoid the numerical instability, here, we are to suggest the performance index as in the following form

$$\Im = [\boldsymbol{w}(\boldsymbol{n}) - w(n-1)]^{\mathrm{T}}[\boldsymbol{w}(\boldsymbol{n}) - \boldsymbol{w}(\boldsymbol{n}-\boldsymbol{1})] + \alpha E[e(n)^2] \quad (16)$$

where $E[\cdot]$ is the expectation operator and α implies the ratio between the change rate of tap weights and the tracking error, and $E[e(n)^2]$ has the following form

$$\begin{aligned} E[e(n)^2] &= E[q_d[n]^2 + \boldsymbol{w}(\boldsymbol{n})^{\mathrm{T}}\boldsymbol{x}_{\boldsymbol{nor}}(\boldsymbol{n})\boldsymbol{x}_{\boldsymbol{nor}}(\boldsymbol{n})^{\mathrm{T}}\boldsymbol{w}(\boldsymbol{n}) \\ &\quad - 2q_d[n]\boldsymbol{x}_{\boldsymbol{nor}}(\boldsymbol{n})^{\mathrm{T}}\boldsymbol{w}(\boldsymbol{n})] \\ &= E[q_d[n]^2] + \boldsymbol{w}(\boldsymbol{n})^{\mathrm{T}}E[\boldsymbol{x}_{\boldsymbol{nor}}(\boldsymbol{n})\boldsymbol{x}_{\boldsymbol{nor}}(\boldsymbol{n})^{\mathrm{T}}]\boldsymbol{w}(\boldsymbol{n}) \\ &\quad - 2E[q_d[n]\boldsymbol{x}_{\boldsymbol{nor}}(\boldsymbol{n})^{\mathrm{T}}]\boldsymbol{w}(\boldsymbol{n}) \\ &= E[q_d[n]^2] + \boldsymbol{w}(\boldsymbol{n})^{\mathrm{T}}\boldsymbol{R}(\boldsymbol{n})\boldsymbol{w}(\boldsymbol{n}) - 2\boldsymbol{p}(\boldsymbol{n})^{\mathrm{T}}\boldsymbol{w}(\boldsymbol{n}) \end{aligned} \quad (17)$$

in which the definitions of auto-correlation matrix and cross-correlation vector are introduced as follows

$$R(n) = E[\boldsymbol{x}_{\boldsymbol{nor}}(\boldsymbol{n})\boldsymbol{x}_{\boldsymbol{nor}}(\boldsymbol{n})^{\mathrm{T}}] \in \Re^{3\times 3}$$
$$p(n) = E[q_d[n]\boldsymbol{x}_{\boldsymbol{nor}}(\boldsymbol{n})] \in \Re^{3}$$

Now, we are to suggest the Lagrangian function with a constraint ($q_d[n] = \boldsymbol{w}(\boldsymbol{n})^{\mathrm{T}}\boldsymbol{x}_{\boldsymbol{nor}}(\boldsymbol{n})$) as follows

$$L(\boldsymbol{w}(\boldsymbol{n}), \lambda) = \frac{1}{2}\Im + \lambda(q_d[n] - \boldsymbol{w}(\boldsymbol{n})^{\mathrm{T}}\boldsymbol{x}_{\boldsymbol{nor}}(\boldsymbol{n})) \quad (18)$$

where λ is a Lagrange multiplier. By taking the derivatives with respect to $\boldsymbol{w}(\boldsymbol{n})$ and λ, we can obtain the following

$$\frac{\partial L}{\partial \boldsymbol{w}(\boldsymbol{n})} = \boldsymbol{w}(\boldsymbol{n}) - \boldsymbol{w}(\boldsymbol{n}-\boldsymbol{1}) + \alpha\boldsymbol{R}(\boldsymbol{n})\boldsymbol{w}(\boldsymbol{n}) - \alpha\boldsymbol{p}(\boldsymbol{n}) - \lambda\boldsymbol{x}_{\boldsymbol{nor}}(\boldsymbol{n}) = 0$$
$$\frac{\partial L}{\partial \lambda} = q_d[n] - \boldsymbol{w}(\boldsymbol{n})^{\mathrm{T}}\boldsymbol{x}_{\boldsymbol{nor}}(\boldsymbol{n}) = 0$$

Let us rearrange above equations into a matrix–vector equation as follows

$$\begin{bmatrix} \boldsymbol{I} + \alpha\boldsymbol{R}(\boldsymbol{n}) & \boldsymbol{x}_{\boldsymbol{nor}}(\boldsymbol{n}) \\ \boldsymbol{x}_{\boldsymbol{nor}}(\boldsymbol{n})^{\mathrm{T}} & 0 \end{bmatrix}\begin{bmatrix} \boldsymbol{w}(\boldsymbol{n}) \\ -\lambda \end{bmatrix} = \begin{bmatrix} \boldsymbol{w}(\boldsymbol{n}-\boldsymbol{1}) + \alpha\boldsymbol{p}(\boldsymbol{n}) \\ q_d[n] \end{bmatrix} \quad (19)$$

where $\boldsymbol{I} \in \Re^{3\times 3}$ is an identity matrix. An inverse matrix of the above equation can be symbolically found in [25] as follows

$$\begin{bmatrix} \boldsymbol{I} + \alpha\boldsymbol{R}(\boldsymbol{n}) & \boldsymbol{x}_{\boldsymbol{nor}}(\boldsymbol{n}) \\ \boldsymbol{x}_{\boldsymbol{nor}}(\boldsymbol{n})^{\mathrm{T}} & 0 \end{bmatrix}^{-1}$$
$$= \begin{bmatrix} \boldsymbol{W}(\boldsymbol{n}) - \boldsymbol{W}(\boldsymbol{n})\boldsymbol{x}_{\boldsymbol{nor}}(\boldsymbol{n})\boldsymbol{y}(\boldsymbol{n})\boldsymbol{x}_{\boldsymbol{nor}}(\boldsymbol{n})^{\mathrm{T}}\boldsymbol{W}(\boldsymbol{n}) & \boldsymbol{W}(\boldsymbol{n})\boldsymbol{x}_{\boldsymbol{nor}}(\boldsymbol{n})\boldsymbol{y}(\boldsymbol{n}) \\ \boldsymbol{y}(\boldsymbol{n})\boldsymbol{x}_{\boldsymbol{nor}}(\boldsymbol{n})^{\mathrm{T}}\boldsymbol{W}(\boldsymbol{n}) & 1 - \boldsymbol{y}(\boldsymbol{n}) \end{bmatrix}$$

with the following definitions

$$\boldsymbol{W}(\boldsymbol{n}) = [\boldsymbol{I} + \alpha\boldsymbol{R}(\boldsymbol{n}) + \boldsymbol{x}_{\boldsymbol{nor}}(\boldsymbol{n})\boldsymbol{x}_{\boldsymbol{nor}}(\boldsymbol{n})^{\mathrm{T}}]^{-1}$$
$$\boldsymbol{y}(\boldsymbol{n}) = [\boldsymbol{x}_{\boldsymbol{nor}}(\boldsymbol{n})^{\mathrm{T}}\boldsymbol{W}(\boldsymbol{n})\boldsymbol{x}_{\boldsymbol{nor}}(\boldsymbol{n})]^{-1}$$

Since the matrix $\boldsymbol{W}(n)$ and scalar $y(n)$ always exist, we can obtain the exact solution of (19) by using above inverse matrix. Solving this equation gives

$$\begin{aligned} \boldsymbol{w}(\boldsymbol{n}) &= [\boldsymbol{W}(\boldsymbol{n}) - \boldsymbol{W}(\boldsymbol{n})\boldsymbol{x}_{\boldsymbol{nor}}(\boldsymbol{n})\boldsymbol{y}(\boldsymbol{n})\boldsymbol{x}_{\boldsymbol{nor}}(\boldsymbol{n})^{\mathrm{T}}\boldsymbol{W}(\boldsymbol{n})] \\ &\quad \times [\boldsymbol{w}(\boldsymbol{n}-\boldsymbol{1}) + \alpha\boldsymbol{p}(\boldsymbol{n})] + \boldsymbol{W}(\boldsymbol{n})\boldsymbol{x}_{\boldsymbol{nor}}(\boldsymbol{n})\boldsymbol{y}(\boldsymbol{n})q_d[n] \end{aligned} \quad (20)$$

Also, by rearranging the above equation, we can obtain the following

$$\begin{aligned} \therefore \quad \boldsymbol{w}(\boldsymbol{n}) &= \boldsymbol{x}_{\boldsymbol{W}}^{+}(\boldsymbol{n})^{\mathrm{T}}q_d[n] + [\boldsymbol{I} - \boldsymbol{x}_{\boldsymbol{W}}^{+}(\boldsymbol{n})^{\mathrm{T}}\boldsymbol{x}_{\boldsymbol{nor}}(\boldsymbol{n})^{\mathrm{T}}]\boldsymbol{W}(\boldsymbol{n}) \\ &\quad \times [\boldsymbol{w}(\boldsymbol{n}-\boldsymbol{1}) + \alpha\boldsymbol{p}(\boldsymbol{n})] \end{aligned} \quad (21)$$

with the following definition

$$\boldsymbol{x}_{\boldsymbol{W}}^{+}(\boldsymbol{n})^{\mathrm{T}} = \boldsymbol{W}(\boldsymbol{n})\boldsymbol{x}_{\boldsymbol{nor}}(\boldsymbol{n})\boldsymbol{y}(\boldsymbol{n})$$

where $\boldsymbol{x}_{\boldsymbol{W}}^{+}(\boldsymbol{n})^{\mathrm{T}}$ is the right weighted pseudo-inverse of $\boldsymbol{x}_{\boldsymbol{nor}}(\boldsymbol{n})^{\mathrm{T}}$, namely, $\boldsymbol{x}_{\boldsymbol{nor}}(\boldsymbol{n})^{\mathrm{T}}\,\boldsymbol{x}_{\boldsymbol{W}}^{+}(\boldsymbol{n})^{\mathrm{T}} = 1$. As a result, the tap-weight vector is updated by (21) in order to minimise the performance index of (16). After finishing the tap-weight updates during the optimisation process, the elbow joint angle estimates are obtained by using (12) with static tap weights. The following section summarises the entire algorithm for elbow joint angle estimation.

4 Entire algorithm of elbow joint angle estimation

The entire EMG signal processing algorithm for elbow joint angle estimation in real time are summarised as shown in Fig. 4. Firstly, the scaling function is obtained from the following Step 1

Step 1: Scaling function generation process

1.1 Set the condition of external load such as no load, 1, 2 and 3 kg
1.2 Acquire a raw EMG signal during $L = 512$ [samples], keeping a specific angle q_i and load: EMG[n]
1.3 Take the RMS of (1): RMS[n]
1.4 Take the LPF of (2): LPF[n]
1.5 Calculate the average of the LPF of (4): $V_{\mathrm{LPF}}[q_i]$
1.5.1 Set $\mathrm{EMG}_{\mathrm{ref}} = V_{\mathrm{LPF}}[q_i]$, if the specific angle is MORF under no load
1.5.2 Set $\mathrm{EMG}_{\max} = V_{\mathrm{LPF}}[q_i]$, if the specific angle is MROF according to external load
1.6 Take the normalised $V_{\mathrm{nor}}[q_i]$ of (8)

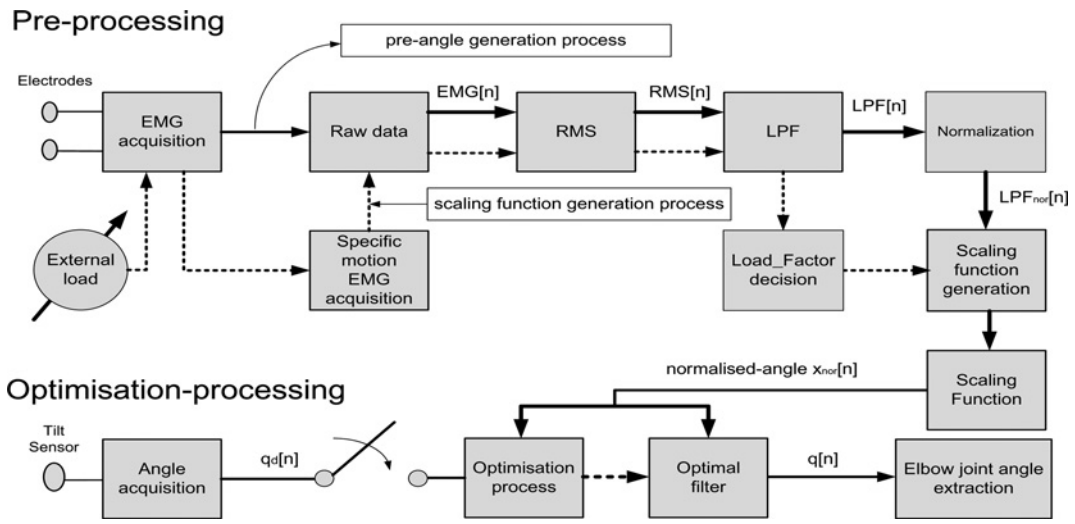

Fig. 4 *Block diagram of entire algorithm*

1.7 Repeat (1.2–1.6) at specific angle such as 0°, 45°, 90° and MORF (here, 145°)
1.8 Determine a_0, a_1, a_2, a_3 of (9) using four q_i angles and the corresponding four $V_{\text{nor}}[q_i]$ values.

Using the coefficients EMG_{ref}, EMG_{max} and a_0, a_1, a_2, a_3, obtained as results of Step 1, we can obtain the normalised angle in real-time using the following Step 2

Step 2: Normalised-angle generation process

2.1 Acquire raw EMG signal in real-time: EMG[n]
2.2 Take RMS of (1): RMS[n]
2.3 Take LPF of (2): LPF[n]
2.4 Calculate the normalised $\text{LPF}_{\text{nor}}[n]$ of (10)
2.5 Obtain the normalised-angle $x_{\text{nor}}[n]$ using (11).

In order to reduce the error between the normalised-angle $x_{\text{nor}}[n]$ and real elbow joint angle $q_d[n]$, we implement the following optimisation process of Step 3

Step 3: Optimisation process

3.1 Initialise tap weight of (13) as a zero vector
3.2 Obtain the error of (15) by using real elbow-joint angle $q_d[n]$ and normalised-angle $x_{\text{nor}}[n]$
3.3 Update the tap weights using (21)
3.4 Repeat (3.2–3.3) for 1024 [samples]

After the tap weights are updated, finally the elbow-joint angle estimate $q[n]$ of (12) is calculated in real time through the entire signal processing as solid lines suggested in Fig. 4. The experimental results are suggested to show the effectiveness of the proposed pre-processing and the optimisation process in the following section.

5 Experimental results

To begin with, the experiment is implemented with a subject who is a normal man (age 28). Then we extend the experiments to multiple subjects. In order to acquire the surface EMG and real elbow joint angle, the QEMG-4 (manufactured by LAXTHA Co.) and EZ-TILT-2000 rev-2 (manufactured by Advanced Orientation Systems, Inc.) are utilised in experiments, respectively. The electrodes are attached to the biceps brachii and triceps brachii of the subject in order to acquire the synergistic EMG signals and the tilt sensor is attached at wrist of the subject. Also, the suitable graphic user interface (GUI) module was developed by using OpenGL and Visual C++ version 6.0. At first, an initialisation is required to implement the suggested algorithm; the initialisation includes obtaining scaling function for the normalised-angle generation and updating tap weights for the elbow joint angle estimate.

5.1 Initialisation

The surface EMG signal is very sensitive according to the environmental conditions, the physical conditions of the subject and the electrode attachment points. Thus, we have to obtain the scaling function in advance for the normalised-angle generation. These procedures were suggested as Step 1 and 2 in the previous section. By using the normalised angle and real elbow joint angle, the optimal tap weights have been updated in Step 3 in the previous section with $\alpha = 1$ as shown in Fig. 5. Fig. 5 shows the updating process of tap weights with no load and an external load, respectively.

5.2 Real-time experiment

After finishing the tap-weight updates, the subject had taken off the tilt sensor attached at one's own wrist, and then we could obtain the experimental results as shown in Figs. 6 and 7. In Figs. 6 and 7, we can see that the elbow joint angle estimate $q[n]$ follows the real angle $q_d[n]$ better than the normalised angle $x_{\text{nor}}[n]$. In order to show the performance improvement by optimisation quantitatively, we have suggested the error L_2-norm values according to the applied external load in Table 1. The data in the table show that the tracking performance using optimisation is superior to ones without using optimisation, although there are a little differences according to the external loads. In addition, we have suggested the snapshots as shown in Fig. 8. From these snapshots, we can know that the virtual arm of GUI module follows the elbow joint motion of the subject well. Also, we could confirm the similar experimental results by repetitive experiments.

doi: 10.1049/iet-spr.2009.0203

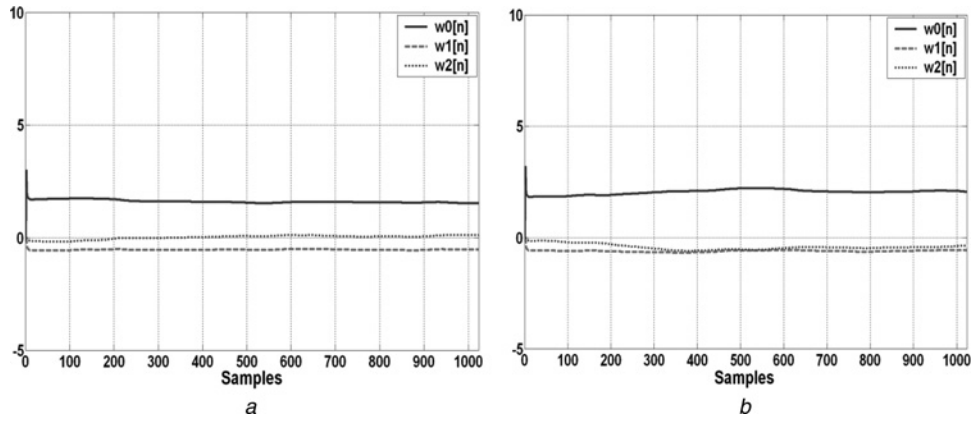

Fig. 5 *Updating tap weights*

a Tap weights with no external load
b Tap weights with external load (3 kgf)

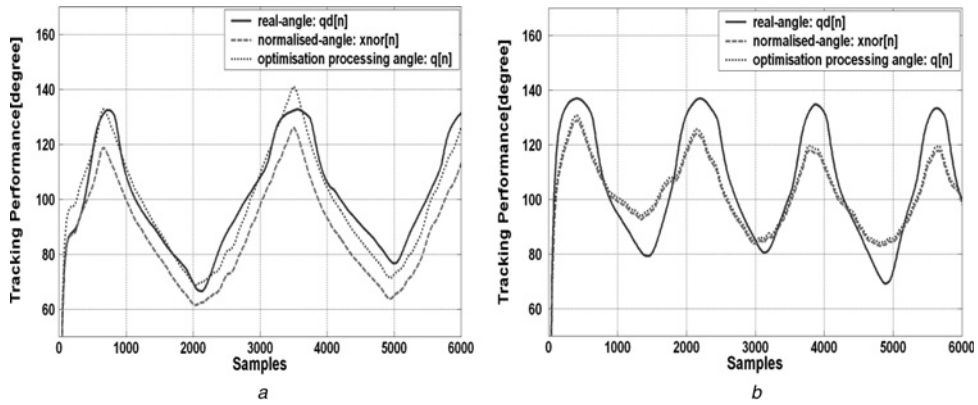

Fig. 6 *Experimental results: elbow angle estimation performance comparison with or without external load*

a No external load
b External load (3 kgf)

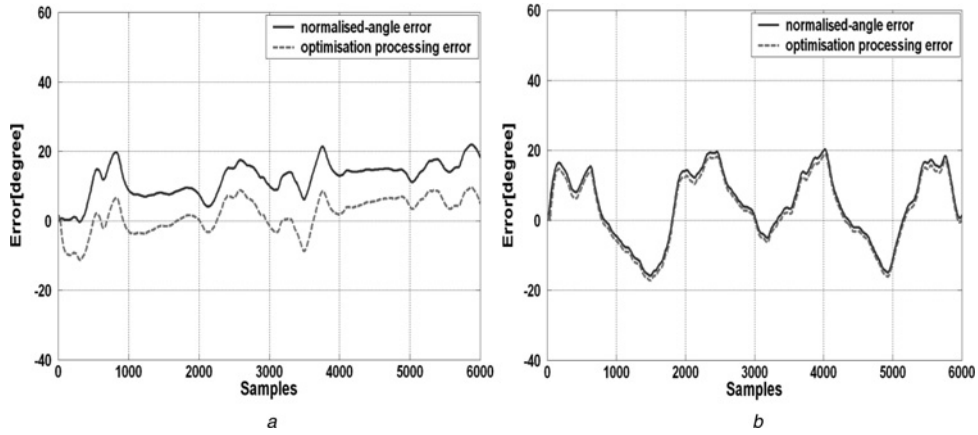

Fig. 7 *Experimental results: error comparisons with or without external load*

a No external load
b External load (3 kgf)

5.3 Extension to multiple subjects

In order to extend the validity of the suggested algorithm, we chose five subjects, one subject is experienced and remaining four subjects are all novices. All subjects are male in their mid-late 20s. Each experiment time was taken 60s with five repetitions. Experiments were performed under the no-load condition. As a result, the L_2-norm error values are shown in Table 2. The experienced subject shows the better performance than novices. Especially, subject C showed a

Table 1 Error L_2-norm comparisons according to the external loads

Applied external load, kgf	0	1	2	3
error ($q_d[n] - x[n]$) before optimisation	2.2153	2.1451	1.0774	1.8623
error ($q_d[n] - q[n]$) after optimisation	0.9749	1.5727	0.9081	1.7603

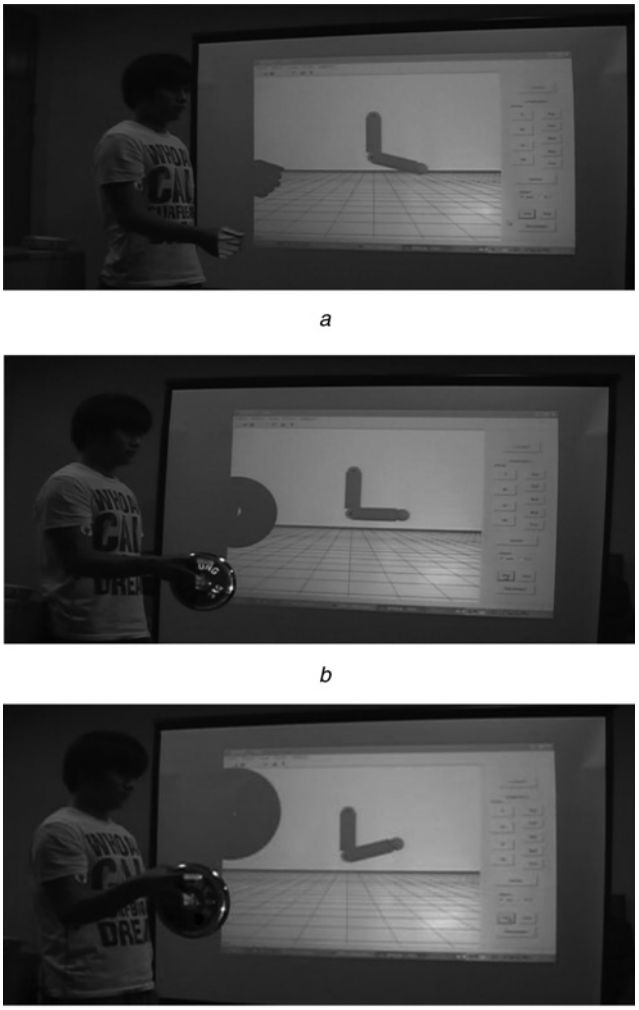

a

b

c

Fig. 8 *Experimental results: snapshots according to the external loads*

a No external load
b Applied external load (2 kgf)
c Applied external load (3 kgf)

Table 2 Error L_2-norm comparisons according to the subjects

Subject	A	B	C	D	E
sex	male	male	male	male	male
age	28	26	25	28	27
experienced/ novice	experienced	novice	novice	novice	novice
error ($q_d[n] - x[n]$) before optimisation	3.1108	6.7934	12.0951	3.9738	6.8376
error ($q_d[n] - q[n]$) after optimisation	1.4883	3.1625	9.5879	2.4166	5.0464

bad performance, although the error must be reduced after applying the optimisation. As we can see in Table 2, most experimental results showed the performance enhancement by the optimisation.

6 Concluding remarks

This paper has suggested the real-time extraction method for a human elbow joint angle by using the EMG signal processing. Actually, we have developed a novel methodology to estimate the human elbow joint angle from the synergistic EMG signals directly, not for the pattern recognition or discrimination in the literatures. The pre-processing and the optimisation processes were proposed in detail based on the assumption that the measured EMG signals are quasi-stationary. Finally, we showed the effectiveness of the suggested algorithm through experiments.

7 Acknowledgments

This work was supported in part by the Mid-career Researcher program through NRF grant funded by the MEST (No. 2008-0061778), and in part by the Ministry of Knowledge Economy (MKE) and Korea Institute for Advancement in Technology (KIAT) through the Workforce Development Program in Strategic Technology, and in part by the MKE under the Human Resources Development program for Convergence Robot Specialists support program supervised by the National IT industry promotion Agency (NIPA) (NIPA-2011-C7000-1001-00051), Republic of Korea.

8 References

1 Rangayyan, R.M.: 'Biomedical signal analysis' (Wiley Inter-Science, 2002)
2 Cavallaro, E., Rosen, J., Perry, J.C., Burns, S., Hannaford, B.: 'Hill-based model as a myoprocessor for a neural controlled powered exoskeleton arm – parameters optimization'. Proc. IEEE Int. Conf. on Robotics and Automation, 2005, pp. 4514–4519
3 Bitzer, S., Der Smagt, P.: 'Learning EMG control of a robotic hand: towards active prostheses'. Proc. IEEE Int. Conf. on Robotics and Automation, 2006, pp. 2819–2823
4 Nishikawa, D., Yu, W., Yokoi, H., Kakazu, Y.: 'EMG prosthetic hand controller using real-time learning method'. Proc. IEEE Int. Conf. on Systems, Man and Cybernetics, October 1999, vol. 1, pp. 153–158
5 Zhao, J., Xie, Z., Jiang, L., Cai, H., Liu, H., Hirzinger, G.: 'Levenberg-Marquardt based neural network control for a five-fingered prosthetic hand'. Proc. IEEE Int. Conf. on Robotics and Automation, 2005, pp. 4482–4487
6 Lee, S.H., Saridis, G.N.: 'The control of a prosthetic arm by EMG pattern recognition', *IEEE Trans. Autom. Control*, 1984, **29**, (4), pp. 290–302
7 Fukuda, O., Tsuji, T., Kaneko, M., Otsuka, A.: 'A human-assisting manipulator teleoperated by EMG signals and arm motions', *IEEE Trans. Robot. Autom.*, 2003, **19**, (2), pp. 210–222
8 Artemiadis, P.K., Kyriakopoulos, K.J.: 'EMG-based teleoperation of a robot arm in planar catching movements using ARMAX model and trajectory monitoring techniques'. Proc. IEEE Int. Conf. on Robotics and Automation, 2006, pp. 3244–3249
9 Morita, S., Shibata, K., Zheng, X.Z., Ito, K.: 'Prosthetic hand control based on torque estimation from EMG signals'. Proc. IEEE/RSJ Int. Conf. on Intelligent Robots and Systems, October 2000, vol. 1, pp. 389–394
10 Su, Y., Fisher, M.H., Wolczowski, A., Bell, G.D., Burn, D.J., Gao, R.X.: 'Towards an EMG-controlled prosthetic hand using a 3-D electromagnetic positioning system', *IEEE Trans. Instrum. Meas.*, 2007, **56**, (1), pp. 178–186
11 Yu, H.-J., Choi, Y.: 'Real-time tracking algorithm of sEMG-based human arm motion'. Proc. IEEE/RSJ Int. Conf. on Intelligent Robots and Systems, 2007, pp. 3416–3421
12 Widrow, B., Mccool, J.M., Glover, J., *et al.*: 'Adaptive noise cancelling: principles and applications', *Proc. IEEE*, 1975, **63**, (12), pp. 1692–1716

doi: 10.1049/iet-spr.2009.0203

13 James, C.J., Hagna, M.T., Jones, R.D., Bones, P.J., Carroll, G.J.: 'Multi-reference adaptive noise canceling applied to the EEG', *IEEE Trans. Biomed. Eng.*, 1997, **44**, (8), pp. 775–779
14 Studer, R.M., de Figueiredo, R.J., Moschytz, G.S.: 'An algorithm for sequential signal estimation and system identification for EMG signals', *IEEE Trans. Biomed. Eng.*, 1984, **31**, (3), pp. 285–295
15 Rittenhouse, D.M., Abdullah, H.A., Runciman, R.J., Basir, O.: 'A neural network model for reconstructing EMG signals from eight shoulder muscles: consequences for rehabilitation robotics and biofeedback', *J. Biomech.*, 2006, **39**, (10), pp. 1924–1932
16 Winter, D.A.: 'Biomechanics and motor control of human movement' (John Wiley & Sons, 1990, 2nd edn.)
17 Doheny, E.P.M., Lowery, M.D., FitzPatrick, P., O'Malley, M.J.: 'Effect of elbow joint angle on force–EMG relationships in human elbow flexor and extensor muscles', *J. Electromyogr. Kinesiol.*, 2008, **18**, pp. 760–770
18 Artemiadis, P.K., Kyriakopoulos, K.J.: 'EMG-based position and force control of a robot arm: application to teleoperation and orthosis'. IEEE/ASME Int. Conf. on Advanced Intelligent Mechatronics, 2007, pp. 1–6
19 Ito, K., Tsuji, T., Kato, A., Ito, M.: 'EMG pattern classification for a prosthetic forearm with three degrees of freedom'. Proc. IEEE Int. Workshop on Robot and Human Communication, 1992, pp. 69–74
20 Fleischer, C., Hommel, G.: 'A human-exoskeleton interface utilizing electromyography', *IEEE Trans. Robot.*, 2008, **24**, (4), pp. 872–882
21 Calvert, T.W., Chapman, A.E.: 'The relationship between the surface EMG and force transients in muscle: simulation and experimental studies', *Proc. IEEE*, 1977, **65**, (5), pp. 682–689
22 Manal, K., Gonzalez, R.V., Lloyd, D.G., Buchanan, T.S.: 'A real-time EMG-driven virtual arm', *Comput. Biol. Med.*, 2002, **32**, pp. 25–36
23 Milner-brown, H.S., Stein, R.B.: 'The relation between the surface electromyogram and muscular force', *J. Physiol.*, 1975, **246**, pp. 549–569
24 Jeon, Y.H.: 'Human anatomy' (in Korean), (Chung Gu Publishing, 2006)
25 Choi, Y., Cheong, J.: 'New expressions of 2X2 block matrix inversion and their application', *IEEE Trans. Autom. Control*, 2009, **54**, (11), pp. 2648–2653